JACS
JOURNAL OF THE AMERICAN CHEMICAL SOCIETY

Communication

pubs.acs.org/JACS

Microtubes with Rectangular Cross-Section by Self-Assembly of a Short β-Peptide Foldamer

Jangbae Kim,[†,+] Sunbum Kwon,[‡,+] Su Hyun Kim,[§] Chung-Kyung Lee,[⊥] Joon-Hwa Lee,[¶] Sung June Cho,[§] Hee-Seung Lee,*[,‡] and Hyotcherl Ihee*[,†]

[†]Institute for Basic Science and [‡]Molecular-Level Interface Research Center, Department of Chemistry, KAIST, Daejeon 305-701, Korea

[§]Department of Applied Chemical Engineering, Chonnam National University, Gwangju 500-757, Korea

[⊥]Division of Magnetic Resonance, Korea Basic Science Institute, Ochang, Chungbuk 363-883, Korea

[¶]Department of Chemistry and Research Institute of Natural Science, Gyeongsang National University, Jinju 660-701, Korea

Supporting Information

ABSTRACT: In nature, complex and well-defined structures are constructed by the self-assembly of biomolecules. It has been shown that β-peptide foldamers can mimic natural peptides and self-assemble into three-dimensional molecular architectures thanks to their rigid and predictable helical conformation in solution. Using shorter foldamers, which can be prepared more easily than longer ones, to form such architectures is highly desirable, but shorter foldamers have been overlooked due to the seemingly inferior number of intramolecular hydrogen bonds to stabilize a folded state in solution. Here we report that a β-peptide tetramer, although it lacks full helical propensity in solution, does self-assemble to form well-defined microtubes with rectangular cross-section by evaporation-induced self-assembly.

Biomolecules often assemble spontaneously and reversibly via combination of multiple noncovalent interactions, and such self-assembly facilitates the organization of higher-order functional nanostructures.[1] Among various types of biomolecules, peptidic scaffolds have attracted much interest due to their biocompatibility and molecular recognition abilities.[2−6] Their physical properties can readily be tuned by precise control of weak interactions between diverse functionalities of side chains. However, direct use of the original scaffolds to build up well-defined, discrete supramolecular architectures has been hampered by the intrinsic flexibility of natural peptides essential for their biological functions and unique enzymatic activities.[7−9] For this reason, many studies on self-assembly of natural peptides involve additional designing of amphiphilic or highly aromatic or cyclic moieties for efficient assemblies.[2−5] By contrast, such additional modification can be bypassed for unnatural β-peptide foldamers because they adopt rigid and predictable secondary structures,[10−12] and thus can be associated into well-defined supramolecular structures.[13−17]

Recently hydrophobic hexa- and heptameric scaffolds of 12-helical β-peptide foldamer have been reported to self-assemble in aqueous solution into highly homogeneous and well-defined molecular architectures with unprecedented three-dimensional (3D) shapes ("foldectures").[17] The unique 3D assemblies of the foldamers were attributed to their intrinsic conformational rigidity which comes from a sufficient number of intramolecular hydrogen bonds (HBs). If shorter foldamers could be used to construct such well-defined foldectures, it would be highly cost-effective in terms of preparation of the building block. However, for much shorter β-peptides with fewer intramolecular HBs to stabilize a folded state, the assembly behavior has not been intensively investigated yet. For example, *trans*-(*S*,*S*)-aminocyclopentanecarboxylic acid tetramer ($ACPC_4$, Scheme 1a) with an N-terminal *tert*-butyloxycarbonyl (Boc) group and a C-terminal benzyl ester is much shorter than the hexamer (7 Å vs 13 Å) and can have only 1.6 helical turns instead of 2.4. In this study, we determine the solution-state conformation and the crystal structure of the specific tetramer[18] and demonstrate a facile route to fabricate rectangular cross-sectioned microtubes via self-assembly. The detailed molecular arrangement of the $ACPC_4$ in a crystal lattice, their interaction patterns, and the solution structure of $ACPC_4$ are resolved by using single-crystal and powder X-ray diffraction (PXRD) and NMR, respectively. The analysis reveals that the tetramer adopts helical conformation in both the tubular assembly and

Scheme 1. (a) Chemical and Crystal Structure of *trans*-(*S*,*S*)-$ACPC_4$ and (b) Schematic Representation of Self-Assembly Process for the Formation of Tubular Morphology

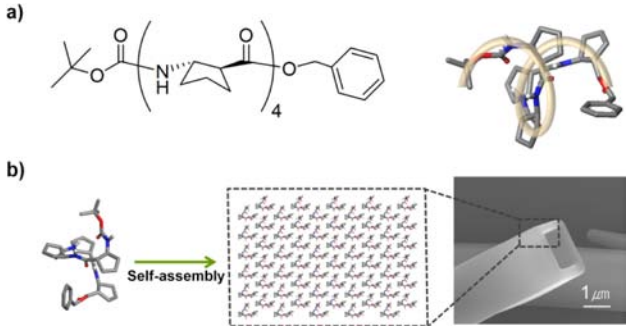

Received: September 6, 2012
Published: December 8, 2012

   dx.doi.org/10.1021/ja3088482 | J. Am. Chem. Soc. 2012, 134, 20573−20576

crystal structure, whereas it lacks full helical propensity in solution.

To verify the solution-state conformation of $ACPC_4$, we performed two-dimensional (2D) NMR study and circular dichroism (CD) analyses at various temperatures. A series of 2D NMR spectra (COSY, TOCSY, and ROESY) of $ACPC_4$ dissolved in pyridine-d_5 were collected at 298 K. As shown in Figure 1a, ROESY data of $ACPC_4$ exhibit a number of

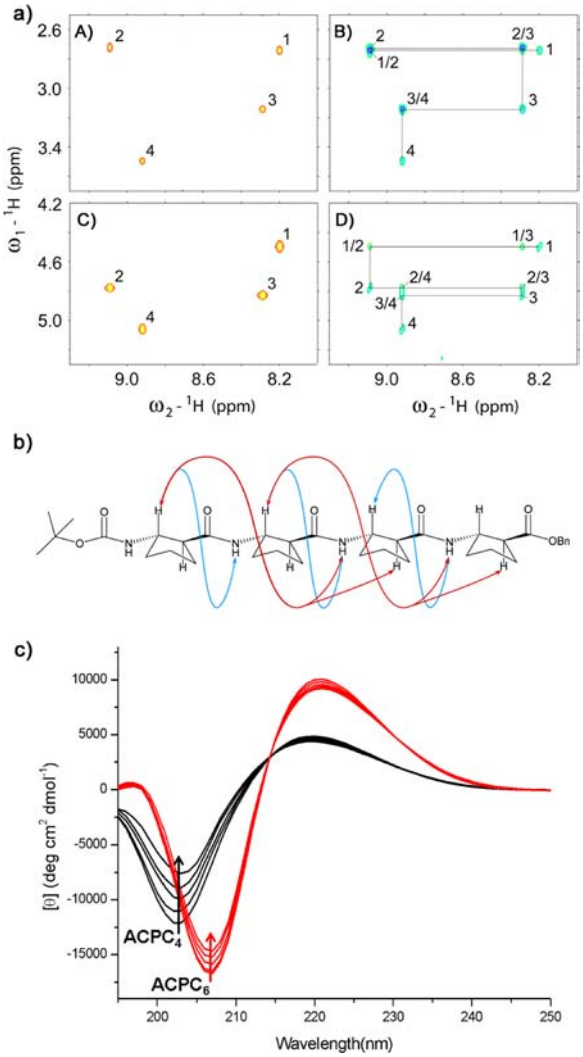

Figure 1. (a) TOCSY (A,C) and ROESY (B,D) 2D NMR spectra of $ACPC_4$ in pyridine-d_5 solution at 298 K. Parts A and B represent the TOCSY and ROESY spectra for the H_α–H_N region, and parts C and D represent the H_β–H_N region of the spectra. (b) Sequential (blue) and medium-range (red) NOEs observed for $ACPC_4$ in ROESY spectrum. (c) Circular dichroism data of *trans*-(*S*,*S*)-$ACPC_4$ (black) and *trans*-(*S*,*S*)-$ACPC_6$ (red) in methanolic solution (1.68 mM) with increasing temperature (20–70 °C at 10 °C intervals).

interresidue NOE cross-peaks that are consistent with the conventional 12-helix, i.e., $H_\beta(i)\leftrightarrow H_N(i+2)$ and $H_\beta(i)\leftrightarrow H_\alpha(i+2)$ (Figure 1b, red line).[19] According to the previous studies by Gellman et al., these medium-range NOEs are typical in 12-helical conformations that have cyclopentyl constraints at the residue level.[20] This result implies that $ACPC_4$ also follows a general folding behavior similar to that of the longer analogues of ACPC homoligomers. On the other hand, there also exist distinctive $H_\beta(i)\leftrightarrow H_N(i+1)$ NOEs between adjacent residues in all possible proton pairs ($H_\beta(1)\leftrightarrow H_N(2)$, $H_\beta(2)\leftrightarrow H_N(3)$, $H_\beta(3)\leftrightarrow H_N(4)$), and those intensities are fairly stronger than those of the longer analogues (Figure 1b, blue line).[19] These sequential NOE correlations suggest that a partially frayed conformation is highly populated along with the well-folded 12-helix in solution. The coexistence of the loosely folded form of $ACPC_4$ in solution is also supported by CD experiments (Figure 1c). The blue shift of the minimum position of the CD spectra of $ACPC_4$ with respect to that of $ACPC_6$ is indicative of the conformational heterogeneity of $ACPC_4$. The CD intensity of $ACPC_4$ is smaller than that of the $ACPC_6$[21,22] and diminishes at a greater rate as temperature increases. These results imply that the 12-helical stability of $ACPC_4$ is weaker and less populated in solution than for the longer analogue. This observation makes it even more interesting to study whether $ACPC_4$ adopts the same secondary structure in the solid state and how it behaves when exposed to self-assembly conditions.

With the conformational information in hand, we performed self-assembly of $ACPC_4$ in various conditions (SI, Figures S1 and S2). The best optimized procedures for the tubular assembly are as follows. Initially, $ACPC_4$ was dissolved in a mixed solvent of methanol (90%) and distilled water (10%), which yielded a transparent solution. Dropping a few microliters of $ACPC_4$ solution on a Si(100) wafer triggered evaporation-induced self-assembly of $ACPC_4$. Under ambient conditions, the solvent vaporized quickly within 5 min, and white precipitate formed on the surface. Scanning electron microscopy (SEM) images reveal formation of rectangular cross-sectioned microtubes in high yield (Figure 2). As shown in Figure 2b, the cross-section of the microtubes displays distinctive rectangular shape. The transmission electron microscopy (TEM) image shows the hollow interior of the microtube morphology (Figure 2c). The outer and inner

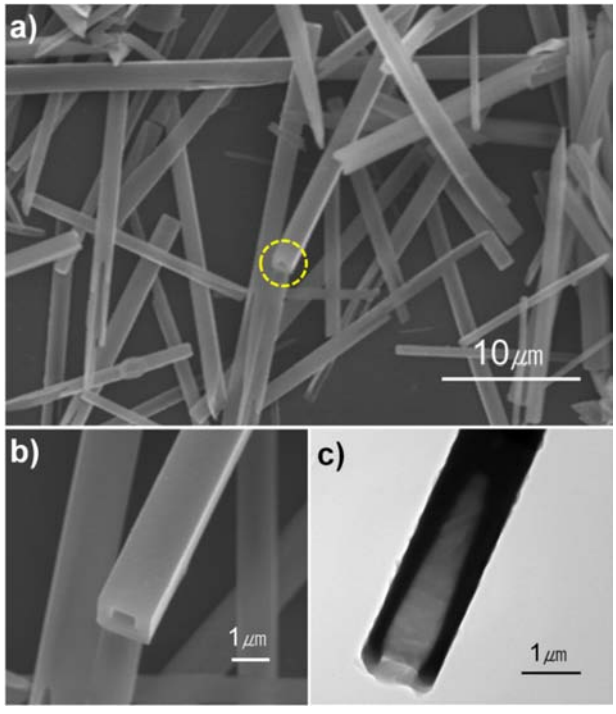

Figure 2. (a) SEM image of $ACPC_4$ microtubes. (b) High-magnification SEM image of the region inside the yellow circle in panel a, indicating rectangular cross-section. (c) TEM image of $ACPC_4$ microtube.

dx.doi.org/10.1021/ja3088482 | J. Am. Chem. Soc. 2012, 134, 20573–20576

diameters of the microtubes are 1.0−1.5 μm and 300−700 nm, respectively, with a wall thickness of ca. 200−400 nm. This is the first example of formation of well-defined rectangular cross-sectioned microtubes by self-assembly of β-peptide building blocks, although some cases with highly aromatic molecules have been reported.[23−25]

To investigate the molecular arrangement of $ACPC_4$ in the tubular assembly by PXRD analysis, some prior structural information of $ACPC_4$ in the solid state is required.[17b,18] Fortunately, we succeeded in obtaining a single crystal of $ACPC_4$ by slow crystallization from a mixed solvent of methanol and water (9:1). The resolved crystal structure has a triclinic symmetry ($P1$) with one $ACPC_4$ molecule in the asymmetric unit (Figures 3a and S3a). The lattice packing of

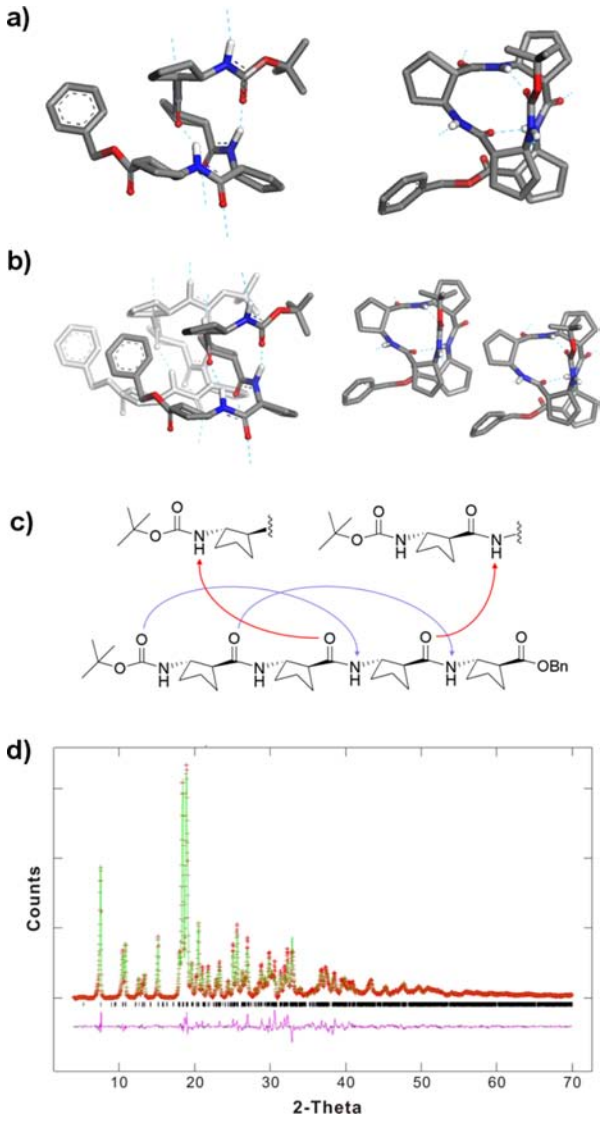

Figure 3. Molecular structure of (a) $ACPC_4$ single crystal and (b) $ACPC_4$ microtubes in the unit cell (left, views perpendicular to helical axes; right, views along the helical axes). (c) Schematic view of intra- (blue) and intermolecular (red) HB patterns. (d) Rietveld refinement patterns for tubular morphologies using PXRD data at 300 K: observed (red crosses), calculated (green solid line), and difference (magenta lower trace). The tic marks (black) indicate the positions of allowed reflections. The 2θ range higher than 24° has been scaled up by a factor of 3 to show more detail.

$ACPC_4$ consists of three kinds of interactions: two intramolecular (1.973 Å, 1.890 Å) and two intermolecular HBs (1.780 Å, 1.789 Å) between the amide hydrogen and the carbonyl oxygen atom in the backbone, and a hydrophobic interaction between the $ACPC_4$ molecules in each layer along the c-direction (Figure S4).

The $ACPC_4$ molecule displays right-handed 12-helical conformation with 1.6 turn (12-membered ring HBs between C═O(i) and N−H(i+3); Figure 3a,c; blue dotted and solid lines), as predicted from the previously known homooligomers of *trans*-ACPC backbone.[21]

The molecular arrangement for tubular structure was solved by using the PXRD technique (Figures 3b and S3b). Details of the PXRD analysis are described in the Supporting Information. The obtained unit cell volume, 1839 $Å^3$, is twice as large as that for a single crystal, 917 $Å^3$ (Table S4). Thus, there are two $ACPC_4$ molecules in the unit cell of the self-assembly, although the same $P1$ space group is maintained (Figure S3b). Rietveld refinement is performed by using the GSAS program suite,[26] and the final result shows a reasonable fitting quality with R_{wp} = 6.57%, R_p = 4.85%, and R_F = 2.98%, as shown in Figure 3d. The detailed structural parameters are listed in Table S5. It is found that the resolved molecular structures of $ACPC_4$ from the Rietveld refinement are essentially identical to the single-crystal structure. When we superpose the refined structure with the single-crystal structure, the atomic root-mean-square distance (RMSD) is measured to be around 0.13 Å.

The molecular packing mode in the tubular assembly suggests that both intermolecular HBs along the helical axes and lateral hydrophobic interactions in polar solvents seem to play important roles in the formation of the specific tubular morphology. When the network buildup was simulated with the intra- and intermolecular HBs taken into account, anisotropic growth of the $ACPC_4$ unit perpendicular to the b axis resulted in the plate-like morphology corresponding to each face of the microtube, as shown in Figure S5. The ordinary $\pi-\pi$ stacking interaction does not seem to play a critical role because the distance between benzyl groups is more than 9.3 Å in the assembly. However, the benzyl group, as a hydrophobic bulky space filler, is necessary for the formation of specific microtube morphology which was supported by the self-assembly of $ACPC_4$ analogues (Figure S6).

To elucidate the formation mechanism of microtubes, we monitored the whole assembly process as a function of time by optical microscopy (Figure S7). At the initial stage of solvent evaporation, the nucleation is initiated from the circumference of the Si wafer (Figure S7a). When the concentrated $ACPC_4$ solution approaches supersaturation via solvent evaporation, the solution turns turbid, indicating a rapid assembly of the $ACPC_4$ into many tiny nucleates. As the evaporation proceeds, a number of rod-like structures grow from the nucleate particles, which generate urchin-like radial bundles (Figure S7b). Until the complete evaporation of solvent, longitudinal growth continues to form rectangular cross-sectioned microtubes, and some of the large microtubes are broken and separated from the radial bundles (Figure S7c,d). The broken part at one end is presumably responsible for the microtube structure having non-identical ends. On the basis of these observations, we propose that the diffusion-limited crystal growth suggested by Eddleston et al. is operational in our case.[27] Without any agitation, mass transport on the growing crystal is diffusion-limited, so the site-dependent growth rate occurs on the crystal face. Mass transport of solute on outside

dx.doi.org/10.1021/ja3088482 | J. Am. Chem. Soc. 2012, 134, 20573−20576

apexes is easier than that in the central region, and faster growth at the outward edges generates a shallow cavity.[28] A central depression on the growing crystal face increasingly depletes solute concentration inside but accelerates growth of edges to give tubular structure (Figure S7e). Similar phenomena of tubular crystallization of organic molecules by evaporation on surfaces have been reported.[27,29]

In summary, β-peptide microtubes with rectangular cross-sections are prepared by the evaporation-induced self-assembly of $ACPC_4$ in a mixed solvent. The single-crystal structure of $ACPC_4$ adopts the right-handed 12-helical conformation via intra- and intermolecular HBs. Rietveld refinement of the experimental PXRD pattern for the microtubes reveals that the tubular foldectures have two $ACPC_4$ molecules in the unit cell, and they also adopt 12-helical conformations maintained by intra- and intermolecular HBs, similar to the single-crystal structure. In this work, we show that a very short non-natural peptide unit can also be used to build up a well-defined, microsized object that may find potential applications in bioengineering or therapeutics such as drug delivery.[30] We hope that our results stimulate this field so that other candidate building blocks that have been neglected because of their short length can be explored in the future.

■ ASSOCIATED CONTENT

Supporting Information

Experimental procedures and additional figures, characterizations, and CIF files. This material is available free of charge via the Internet at http://pubs.acs.org.

■ AUTHOR INFORMATION

Corresponding Author

hee-seung_lee@kaist.ac.kr; hyotcherl.ihee@kaist.ac.kr

Author Contributions

[+]J.K. and S.K. contributed equally.

Notes

The authors declare no competing financial interest.

■ ACKNOWLEDGMENTS

This research was supported by Basic Science Research Program through the National Research Foundation of Korea, funded by the Ministry of Education, Science and Technology (grants 2012-0000908, 2011-0012141), and the Research Center Program of Institute for Basic Science.

■ REFERENCES

(1) Whitesides, G. M.; Mathias, J. P.; Seto, C. T. *Science* **1991**, *254*, 1312.
(2) Hartgerink, J. D.; Beniash, E.; Stupp, S. I. *Science* **2001**, *294*, 1684.
(3) Zhang, S. *Nat. Biotechnol.* **2003**, *21*, 1171.
(4) Reches, M.; Gazit, E. *Science* **2003**, *300*, 625.
(5) Ghadiri, M. R.; Granja, J. R.; Milligan, R. A.; McRee, D. E.; Khazanovich, N. *Nature* **1993**, *366*, 324.
(6) Görbitz, C. H. *Chem.—Eur. J.* **2001**, *7*, 5153.
(7) Bellesia, G.; Shea, J.-E. *J. Chem. Phys.* **2009**, *131*, 111102.
(8) Henzler-Wildman, K.; Kern, D. *Nature* **2007**, *450*, 964.
(9) Huang, F.; Nau, W. M. *Angew. Chem., Int. Ed.* **2003**, *42*, 2269.
(10) Gellman, S. H. *Acc. Chem. Res.* **1998**, *31*, 173.
(11) Cheng, R. P.; Gellman, S. H.; DeGrado, W. F. *Chem. Rev.* **2001**, *101*, 3219.
(12) Goodman, C. M.; Choi, S.; Shandler, S.; DeGrado, W. F. *Nat. Chem. Biol.* **2007**, *3*, 252.
(13) Daniels, D. S.; Petersson, J.; Qiu, J. X.; Schepartz, A. *J. Am. Chem. Soc.* **2007**, *129*, 1532.
(14) Martinek, T. A.; Hetényi, A.; Fülöp, L.; Mándity, I. M.; Tóth, G. K.; Dékány, I.; Fülöp, F. *Angew. Chem., Int. Ed.* **2006**, *45*, 2396.
(15) Pomerantz, W. C.; Yuwono, V. M.; Pizzey, C. L.; Hartgerink, J. D.; Abbott, N. L.; Gellman, S. H. *Angew. Chem., Int. Ed.* **2008**, *47*, 1241.
(16) Pomerantz, W. C.; Yuwono, V. M.; Drake, R.; Hartgerink, J. D.; Abbott, N. L.; Gellman, S. H. *J. Am. Chem. Soc.* **2011**, *133*, 13604.
(17) (a) Kwon, S.; Jeon, A.; Yoo, S. H.; Chung, I. S.; Lee, H.-S. *Angew. Chem., Int. Ed.* **2010**, *49*, 8232. (b) Kwon, S.; Shin, H. S.; Gong, J.; Eom, J.-H.; Jeon, A.; Yoo, S. H.; Chung, I. S.; Cho, S. J.; Lee, H.-S. *J. Am. Chem. Soc.* **2011**, *133*, 17618. (c) Kwon, S.; Kang, K.; Jeon, A.; Park, J. H.; Choi, I. S.; Lee, H.-S. *Tetrahedron* **2012**, *68*, 4368.
(18) Although previous studies on the related tetramer formed from ACPC subunits suggested that a tetramer can adopt 12-helical conformation, the independent conformational analyses in this study were inevitable because the direct use of previous structural information was not possible. See: (a) Choi, S. H.; Guzei, I. A.; Spencer, L. C.; Gellman, S. H. *J. Am. Chem. Soc.* **2010**, *132*, 13879. (b) Abraham, E.; Bailey, C. W.; Claridge, T. D. W.; Davies, S. G.; Ling, K. B.; Odell, B.; Rees, T. L.; Roberts, P. M.; Russell, A. J.; Smith, A. D.; Smith, L. J.; Storr, H. R.; Sweet, M. J.; Thompson, A. L.; Thomson, J. E.; Tranter, G. E.; Watkin, D. J. *Tetrahedron: Asymmetry* **2010**, *21*, 1797.
(19) Barchi, J. J.; Huang, X.; Appella, D. H.; Christianson, L. A.; Durell, S. R.; Gellman, S. H. *J. Am. Chem. Soc.* **2000**, *122*, 2711.
(20) Wang, X.; Espinosa, J. F.; Gellman, S. H. *J. Am. Chem. Soc.* **2000**, *122*, 4821.
(21) Appella, D. H.; Christianson, L. A.; Klein, D. A.; Powell, D. R.; Huang, X.; Barchi, J. J.; Gellman, S. H. *Nature* **1997**, *387*, 381.
(22) Appella, D. H.; Christianson, L. A.; Klein, D. A.; Richards, M. R.; Powell, D. R.; Gellman, S. H. *J. Am. Chem. Soc.* **1999**, *121*, 7574.
(23) Zhao, Y. S.; Xu, J.; Peng, A.; Fu, H.; Ma, Y.; Jiang, L.; Yao, J. *Angew. Chem., Int. Ed.* **2008**, *47*, 7301.
(24) Zhang, X.; Zhang, X.; Shi, W.; Meng, X.; Lee, C.; Lee, S.-T. *Angew. Chem., Int. Ed.* **2007**, *46*, 1525.
(25) Yoon, S. M.; Hwang, I.-C.; Kim, K. S.; Choi, H. C. *Angew. Chem., Int. Ed.* **2009**, *48*, 2506.
(26) Larson, A. C.; Von Dreele, R. B. General Structure Analysis System (GSAS); Los Alamos National Laboratory Report LAUR 86-748, 2004.
(27) Eddleston, M. D.; Jones, W. *Cryst. Growth Des.* **2010**, *10*, 365.
(28) Nanev, C. N. *Prog. Cryst. Growth Charact. Mater.* **1997**, *35*, 1.
(29) Seo, M.; Seo, G.; Kim, S. Y. *Angew. Chem., Int. Ed.* **2006**, *45*, 6306.
(30) (a) Cui, H.; Muraoka, T.; Cheetham, A. G.; Stupp, S. I. *Nano Lett.* **2009**, *9*, 945. (b) Bella, A.; Ray, S.; Shaw, M.; Ryadnov, M. G. *Angew. Chem., Int. Ed.* **2012**, *51*, 428.